Available online at www.sciencedirect.com
SCIENCE DIRECT
Polymer 47 (2006) 897–906
polymer
www.elsevier.com/locate/polymer

Discrete bond-weighted random scission of linear polymers

J.E.J. Staggs

Energy Resources Research Institute, University of Leeds, Leeds LS2 9JT, UK

Received 4 October 2005; received in revised form 28 November 2005; accepted 29 November 2005
Available online 22 December 2005

Abstract

A discrete population balance model, where the probabilities of particular bonds breaking within a given mer are assigned individual weights, is studied. The model represents an extension of previous population balance models and provides a framework for the analysis of a number of different scission mechanisms including pure random scission, end-chain scission, simultaneous random and end-chain scission and break-at-a-point scission. The main thrust of the work is aimed at interpreting observed degradation rates of PMMA. The model suggests that both random and end-chain scission must occur in order to reproduce the observed dependence of degradation rate with initial degree of polymerisation at low temperatures. However, at high temperatures it was found that molecule size dependence must also be incorporated in order to explain the observed behaviour.

Keywords: Thermal degradation; Population balance model; Random scission

1. Introduction

Accurate and well founded theoretical descriptions of the thermal degradation mechanisms of solid polymers are vital in numerous research areas including chemical recycling applications, and fire and combustion science. Not only is it important to be able to predict degradation and volatilisation rates for a variety of heating conditions, it is also important to be able to predict the composition of the volatile products.

The last 10 years has seen an increase in the effort of researchers to develop new mathematical models of particular degradation mechanisms for polymers, such as random scission and end-chain scission, based on population balance equations. In this approach, the population of polymer molecules is either viewed as a collection of chains of infinitely variable length, which may break at any point (continuous models) or as a set of molecules, which may break at only a finite number of locations (discrete models). A specific scission mechanism is then applied to the population of molecules, resulting in either an integro-differential equation or a set of ordinary differential equations describing the evolution of the frequency distribution, depending on whether the continuous or discrete view of the molecular spectrum is employed. In general, the discrete modelling approach is probably preferable, as it more closely resembles the actual bond breaking process. However, the continuous approach is often more convenient and more tractable for analysis. The drawback of the population balance approach is that convenient, closed-form solutions for the frequency distributions are elusive and so one is often forced to rely on numerical solutions, which may require considerable effort to achieve.

McCoy and co-workers [1–5] have led the way in the development of continuous population balance models and as a result of their work much insight into these processes has been gained. In a recent paper [6], the author analysed a continuous model for random scission with recombination and presented the general solutions of the continuous random scission model and the continuous recombination model. Discrete models have also been successfully applied in a number of situations and references [7–11] are a representative but incomplete selection. Finally, the other approach qualifying for inclusion in this brief overview involves the use of Monte-Carlo-type methods to model polymerisation and degradation of polymers [12–14]. These methods have been shown to agree well with models based on population balance equations for random scission, end-chain scission and recombination [8,9].

This paper presents an extension of previous discrete population balance models, and analyses the case where individual weights may be assigned to each bond within a particular linear molecule. As will be seen, this framework encompasses models for random scission as well as end-chain scission and new insights into these processes are presented.

E-mail address: fuejejs@leeds.ac.uk

0032-3861/$ - see front matter © 2005 Elsevier Ltd. All rights reserved.
doi:10.1016/j.polymer.2005.11.085

It will also be used to analyse the case of simultaneous random and end-chain scission, which is thought to be important in the thermal degradation of PMMA [15–18]. The analysis of other scission mechanisms is also possible within this framework and the break-at-a-point model is briefly presented and investigated.

For brevity, the following abbreviations are used below: RS (random scission), ECS (end-chain scission), UID (uniform initial distribution) and TG (thermogravimetric).

2. The general bond-weighted model

Consider a population of molecules containing N_i i-mers, $i=1, 2\ldots n$. Let the relative probability of bond j breaking within an i-mer be $w_j^{(i)}$, so that $\sum_{j=1}^{i-1} w_j^{(i)} = 1$. Furthermore, let the total number of molecules in the population be $N = \sum_{i=1}^{n} N_i$. Assuming that the rate at which bonds break in a group of i-mers is proportional to the number of bonds in the group and that no molecules are removed from the population, then in time step Δt, the expected number of j-mers and $(i-j)$-mers formed from the scission of bond j in a population of i-mers will be $k_i(i-1)w_j^{(i)}N_i\Delta t$, where k_i is the temperature dependent degradation rate for bond-breaking in an i-mer. Now, i-mers will be formed by the scission of bonds $j-i$ and i in a j-mer with $j>i$. Consequently, the expected number of i-mers formed from scissions in larger molecules in time step Δt will be $\sum_{j=i+1}^{n} k_j(j-1)(w_{j-i}^{(j)} + w_i^{(j)})N_j\Delta t$. Therefore, the evolution of the population will be governed by the system of linear ordinary differential equations

$$\frac{\mathrm{d}N_i}{\mathrm{d}t} = \begin{cases} -k_i(i-1)N_i & \\ +\sum_{j=i+1}^{n} k_j(j-1)\left(w_{j-i}^{(j)} + w_i^{(j)}\right)N_j, & i = 1,2,...,n-1 \\ -k_n(n-1)N_n, & i = n \end{cases} \tag{1}$$

with initial conditions $N_i(0)/N(0) = \nu_i$. Here ν_i is the fraction of i-mers in the initial population. In reality it is likely that the symmetry $w_i^{(j)} = w_{j-i}^{(j)}$ will be valid. However, as no significant simplification of the analysis results from this observation, it will not be employed.

For simplicity the process of recombination, where a j-mer and an $(i-j)$-mer combine to form an i-mer, will be neglected, although there are no insurmountable practical difficulties in incorporating this process into the current model. If the rate at which recombination occurs to form i-mers is $k_i^{(r)}$, then the modified model equations will be [9]

$$\frac{\mathrm{d}N_i}{\mathrm{d}t} = \begin{cases} -k_1^{(r)}N_1 + \sum_{j=2}^{\infty} k_j(j-1)\left(w_{j-1}^{(j)} + w_1^{(j)}\right)N_j, & i = 1 \\ -\left(k_i(i-1) + k_i^{(r)}\right)N_i & \\ +\sum_{j=i+1}^{\infty} k_j(j-1)\left(w_{j-i}^{(j)} + w_i^{(j)}\right)N_j & \\ +\frac{k_i^{(r)}}{2N}\sum_{j=1}^{i-1} N_jN_{i-j}, & i > 1 \end{cases} \tag{2}$$

However, the increased level of complexity of including this feature reduces the amount of analysis possible without recourse to numerical solutions. Two earlier papers [6,9] consider the effect of recombination on models of pure random scission and end-chain scission.

The general solution of the bond-weighted model can be written down for isothermal conditions using the upper-triangular structure of the system. Without going into detail, it is

$$\frac{N_i}{N(0)} = \begin{cases} \nu_1 + \sum_{j=2}^{n} \kappa_j\Omega_{1j}\int_0^t \frac{N_j(t')}{N(0)}\mathrm{d}t', & i = 1 \\ \nu_i\mathrm{e}^{-\kappa_i t} + \sum_{j=i+1}^{n} \kappa_j\Omega_{ij}\int_0^t \frac{N_j(t')}{N(0)}\mathrm{d}t', & i = 2,\ldots,n-1 \\ \nu_n\mathrm{e}^{-\kappa_n t}, & i = n \end{cases} \tag{3}$$

Here $K_i = (i-1)k_i$ and $\Omega_{ij} = w_{j-i}^{(j)} + w_i^{(j)}$. For simplicity in what follows, we shall assume that each k_i has the same value k, which is also assumed to be of Arrhenius form $k(T) = \exp(J - T_A/T)$ where J is the logarithm of the pre-exponential factor and T_A is the activation temperature. Also if we define dimensionless time τ by

$$\tau = \int_0^t k(T(t'))\mathrm{d}t' \tag{4}$$

then this enables us to develop solutions in terms of τ that are valid for any heating conditions. Once these have been found, they may be compared with experimental results by calculating t from the solution of $\mathrm{d}\tau/\mathrm{d}t = k(T(t))$, $\tau(0) = 0$.

2.1. Moments

The mth moment of the distribution μ_m is defined as $\mu_m = \sum_{i=1}^{n} i^m N_i$ and it can easily be shown that

$$\frac{\mathrm{d}\mu_m}{\mathrm{d}\tau} = \sum_{j=1}^{n} S_j^{(m)}N_j \tag{5}$$

where $S_j^{(m)} = (j-1)\sum_{i=1}^{j-1}(i^m + (j-i)^m - j^m)w_i^{(j)}$. Now, in particular, we note that when $m=1$, $S_j^{(1)} = 0$ for all j and so it follows that the first moment μ_1 (proportional to the total mass of the distribution) is constant if no molecules are removed. Furthermore when $m=0$, we have that $S_j^{(0)} = j-1$ (since

$\sum_{j=1}^{i-1} w_j^{(i)} = 1$) and so it follows that

$$\frac{d\mu_0}{d\tau} = \sum_{j=1}^{n}(j-1)N_j = \mu_1 - \mu_0 \tag{6}$$

The solution of this first order differential equation gives the evolution of the total number of molecules in the population $N = \mu_0$:

$$\frac{N}{N(0)} = \chi_0 - (\chi_0 - 1)e^{-\tau} \tag{7}$$

where $\chi_0 = \mu_1/N(0)$ is the initial number-average degree of polymerisation of the population.

The number-average degree of polymerisation χ (equal to the relative number-average molecular mass $M_1 = \mu_1/\mu_0$) will be given by

$$\chi = \frac{1}{1-(1-1/\chi_0)e^{-\tau}} \tag{8}$$

which indicates a linear relationship $1/\chi - 1/\chi_0 \sim (1-1/\chi_0)\tau$ between $1/\chi$ and τ for small τ (or large χ). The relative weight-average molecular mass $M_2 = \mu_2/\mu_1$ and the polydispersity $\eta = M_2/M_1$ will depend on the specific molecular bond weights $w_i^{(j)}$.

2.2. Volatilisation

For some applications, such as predicting volatilisation rates, it is necessary to quantify the rate at which gaseous products evolve. Some authors [3] have attempted to employ relatively detailed mass transfer processes, however, following the approach of earlier papers [6,8,9], we shall adopt the simplest possible description, i.e. there exists a characteristic number of repeat units m_v below which polymer molecules are volatile. With this in mind, let the mth partial moment $\mu_m^{(j)}$ of the frequency distribution be defined as

$$\mu_m^{(j)}(\tau) = \sum_{i=j}^{n} i^m N_i(\tau) \tag{9}$$

The fraction of remaining mass to initial mass will then be approximated by $\mu_1^{(m_v)}(\tau)/\mu_1$.

3. Specific scission mechanisms

3.1. Pure random scission

For pure RS, each bond within a molecule is equally likely to break and consequently $w_i^{(j)} = 1/(j-1)$. This case, relevant for the thermal degradation of polymers such as polyethylene, has already been dealt with extensively in the literature [3,6,8]. However, it transpires, as will be seen presently, that when χ_0 is large, good approximations for the relative weight-average molecular mass and the polydispersity during degradation may be calculated.

Let $N_i(\tau) = N(\tau)e^{(i-1)\tau}\varphi(\tau)$. Then for large n, we find that φ satisfies the equation

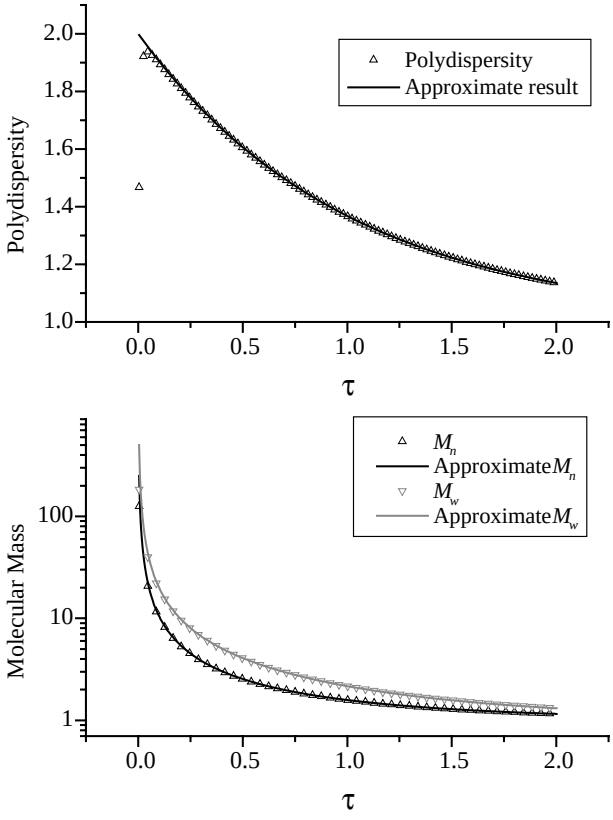

Fig. 1. Comparison between exact and approximate results for polydispersity and molecular mass for random scission.

$$\frac{d\varphi}{d\tau} + \frac{\varphi}{N}\frac{dN}{d\tau} = 2\varphi\sum_{i=1}^{\infty} e^{-i\tau} \tag{10}$$

The summation on the RHS is the infinite sum of a geometric progression, common ratio $e^{-\tau}$ and equals $e^{-\tau}/(1-e^{-\tau})$. Now noting from Eq. (7) that when $\tau > 0$, $dN/d\tau \approx Ne^{-\tau}/(1-e^{-\tau})$, it follows from (10) that an approximate solution, valid when $\tau > 0$ and n is large, is $\varphi \approx 1 - e^{-\tau}$. Hence the relative frequency of i-mers will be given approximately by

$$\frac{N_i(\tau)}{N(\tau)} \approx e^{-(i-1)\tau}(1-e^{-\tau}) \tag{11}$$

Obviously this solution will not be valid initially as it takes no account of the initial distribution of molecules, but we expect it to be increasingly accurate as τ increases, regardless of the initial distribution.

Defining $G(\tau) = 1/(1-e^{-\tau})$, it follows that the mth moment is given approximately by $\mu_m \approx N(\tau)(1-e^{-\tau})\sum_{i=0}^{m} {}^mC_i(-1)^i G^{(i)}$, where ${}^mC_i = m!/(i!(m-i)!)$ is the binomial coefficient and $G^{(i)} = d^iG/d\tau^i$. Therefore, the relative number-average molecular mass M_1, the relative weight-average molecular mass M_2 and the polydispersity η are given approximately by $M_1 \approx 1/(1-e^{-\tau})$, $M_2 \approx (1+e^{-\tau})/(1-e^{-\tau})$ and $\eta \approx 1+e^{-\tau}$. These quantities are compared with the exact results for a UID with $\chi_0 = 250$ in Fig. 1. The approximate results give excellent agreement for all cases except in the vicinity of $\tau = 0$, as expected.

It is possible to show from the population balance equations that when n is large, the zeroth and first partial moments (defined by Eq. (9) above) for pure random scission satisfy the equations

$$\frac{\mathrm{d}\mu_0^{(m_\mathrm{v})}}{\mathrm{d}t} = \mu_1^{(m_\mathrm{v})} - (2m_\mathrm{v}-1)\mu_0^{(m_\mathrm{v})},$$
$$\frac{\mathrm{d}\mu_1^{(m_\mathrm{v})}}{\mathrm{d}t} = -m_\mathrm{v}(m_\mathrm{v}-1)\mu_0^{(m_\mathrm{v})} \tag{12}$$

Assuming that m_v is small enough so that the initial conditions $\mu_0^{(m_\mathrm{v})}(0) = N(0)$, $\mu_1^{(m_\mathrm{v})}(0) = \mu_1$ are valid, it may be easily shown that the solutions of these equations are

$$\frac{\mu_0^{(m_\mathrm{v})}(\tau)}{N(0)} = (\chi_0 - (m_\mathrm{v}-1))\mathrm{e}^{-(m_\mathrm{v}-1)\tau} - (\chi_0 - m_\mathrm{v})\mathrm{e}^{-m_\mathrm{v}\tau} \tag{13}$$

$$\frac{\mu_1^{(m_\mathrm{v})}(\tau)}{\mu_1} = m_\mathrm{v}\left(1-\frac{m_\mathrm{v}-1}{\chi_0}\right)\mathrm{e}^{-(m_\mathrm{v}-1)\tau} - (m_\mathrm{v}-1)\left(1-\frac{m_\mathrm{v}}{\chi_0}\right)\mathrm{e}^{-m_\mathrm{v}\tau} \tag{14}$$

Hence it follows that for large χ_0, instantaneous volatilisation of species with fewer than m_v repeat units implies that the remaining mass will be given approximately by $\mu_1^{(m_\mathrm{v})}/\mu_1 \approx m_\mathrm{v}\mathrm{e}^{-(m_\mathrm{v}-1)\tau} - (m_\mathrm{v}-1)\mathrm{e}^{-m_\mathrm{v}\tau}$. Note that this corresponds to Eq. (18) in Ref. [8] with $r = 1-\mathrm{e}^{-\tau}$. Therefore, we have the remarkable result that for pure random scission, the remaining mass is independent of the shape of the initial molecular distribution. Furthermore, when the initial degree of polymerisation is large, the remaining mass does not depend on the initial distribution at all.

Also, when $m_\mathrm{v} \gg 1$, a good approximation for the remaining mass is $\mu_1^{(m_\mathrm{v})}/\mu_1 \approx \mathrm{e}^{-(m_\mathrm{v}-1)\tau}(1+(m_\mathrm{v}-1)\tau)$. This indicates that if we define $J^* = J + \ln(m_\mathrm{v}-1)$ and $k^* = \exp(J^* - T_\mathrm{A}/T)$, then the remaining mass becomes $\mu_1^{(m_\mathrm{v})}/\mu_1 \approx e^{-\tau}(1+\tau)$, i.e. a function of τ only, as long as we now define τ by $\mathrm{d}\tau/\mathrm{d}k = k^*$.

The graph in Fig. 2 shows a comparison of the model prediction with experimental TG data for polyethylene. The parameters $J^* = 24.06$ and $T_\mathrm{A} = 21{,}616$ K were found from a least squares best fit to the experimental data. The polyethylene was supplied by Polymer Laboratories (UK) inc. with a molecular weight of 2015 g mol^{-1} and a polydispersity of 1.14, part no. 2650-3001, batch no. 26503-1. Although this polymer has the drawback of having a much lighter molecular weight than commercial polymers, it is free of additives, and has few branch points along the molecule. The experiment was conducted in nitrogen at a heating rate of 10 K min^{-1} using a Shimadzu TGA-50 machine with initial sample mass of approximately 8 mg.

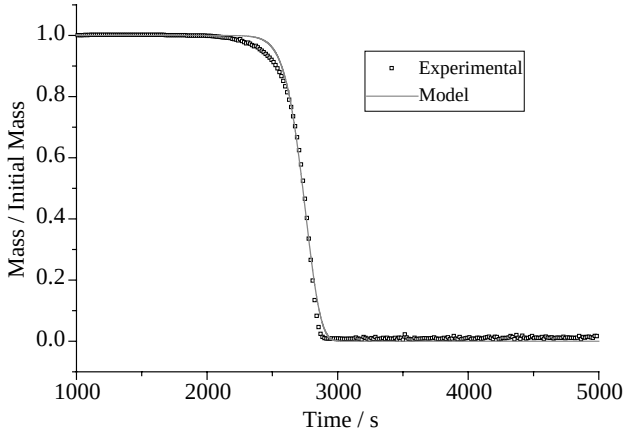

Fig. 2. Comparison of model with constant heating rate TGA.

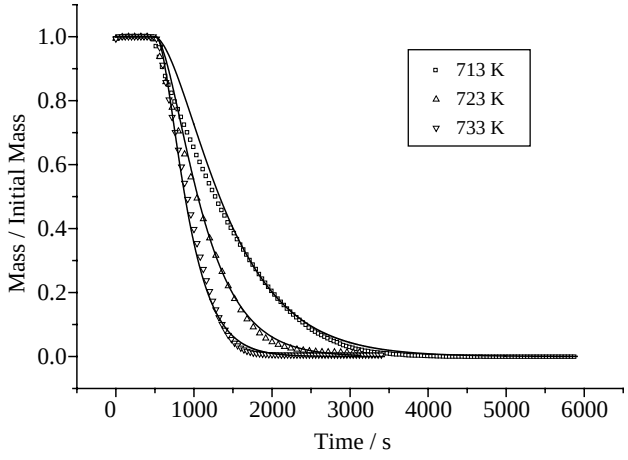

Fig. 3. Isothermal TG comparison with model. Symbols correspond to experimental data and curves to model predictions.

The graph in Fig. 3 compares model predictions using the same values for J^* and T_A found above, with isothermal TG experiments in nitrogen using the same polymer. The desired isothermal temperature was reached by initially increasing the temperature at the TG analyser's greatest rate of 50 K min^{-1}. Note that the initial heating period is also accounted for in the model prediction through Eq. (4). Both this figure and Fig. 2 indicate that the model under predicts the observed mass loss rate at low temperatures, but provides reasonable agreement at moderate and higher temperatures.

3.2. Power law

We now consider an extension of the case above, where there is an increasing probability of a bond breaking as we move from the centre of the molecule to the end. Let the probability of an end bond breaking be λ times the probability of a bond breaking in the middle of the molecule, then applying a power law for the remaining bond weights gives

$$w_i^{(j)} = \frac{1+(\lambda-1)|(2i-j)/(j-2)|^\alpha}{j-1+(\lambda-1)\sigma_j^{(\alpha)}}, \tag{15}$$

$j \geq 3,\ 1 \leq i \leq j-1$

with $w_1^{(2)} = 1, \quad w_1^{(3)} = w_2^{(3)} = 1/2$, and

$$\sigma_j^{(\alpha)} = \sum_{i=1}^{j-1}\left|\frac{2i-j}{j-2}\right|^\alpha, \quad j \geq 3 \tag{16}$$

The graph in Fig. 4 shows some bond weight profiles for a molecule with 250 repeat units for $\alpha = 1, 8, 64$ and $\lambda = 100$. The

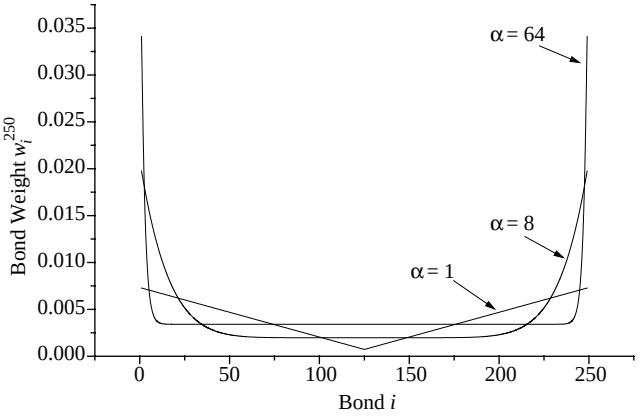

Fig. 4. Example power-law bond weight profiles $w_i^{(j)}$ for $j=250$.

graphs in Figs. 5 and 6 show the effect of α on the relative frequency distributions N_m/N for a UID at specific values of τ for $\lambda=10$.

When $\lambda=1$, or $\alpha=0$, the case of pure RS is recovered. For $j\geq 3$, as $\alpha\to\infty$, $|(2i-j)/(j-2)|^{\alpha}\to 0$ for $1<i<j-1$ and $|(2i-j)/(j-2)|^{\alpha}\to 1$ when $i=1$ or $j-1$. This implies that as $\alpha\to\infty$, $\sigma_j^{(\alpha)}\to 2$, and so an end-bond weighted case is recovered where

$$w_i^{(j)}=\begin{cases}\dfrac{\lambda}{2\lambda+j-3}, & i=1 \text{ or } j-1\\ \dfrac{1}{2\lambda+j-3}, & i=2,3,\ldots j-2\end{cases} \tag{17}$$

This case may be thought of as a mixture of simultaneous RS and ECS, where the probability of an end bond breaking is λ times the probability of an internal bond breaking. The value of λ now determines the relative degree of ECS compared with RS. As $\lambda\to\infty$, we recover the case of pure ECS, given for $j>2$ by

$$w_i^{(j)}=\begin{cases}\dfrac{1}{2}, & i=1 \text{ or } j-1\\ 0, & \text{otherwise}\end{cases} \tag{18}$$

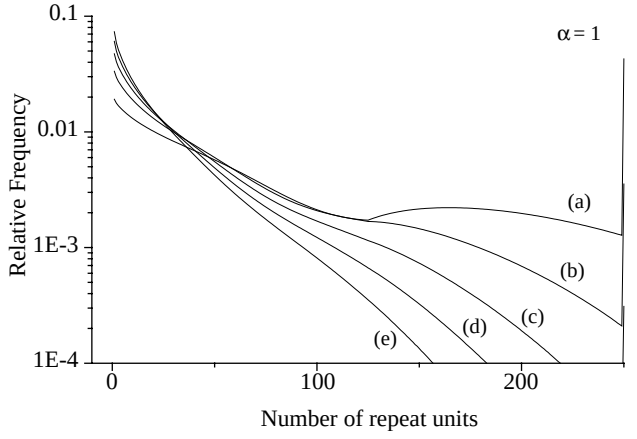

Fig. 5. Frequency distributions for $\alpha=1$, UID with $\chi_0=250$. (a) $\tau=0.008$, (b) $\tau=0.016$, (c) $\tau=0.025$, (d) $\tau=0.033$, (e) $\tau=0.044$.

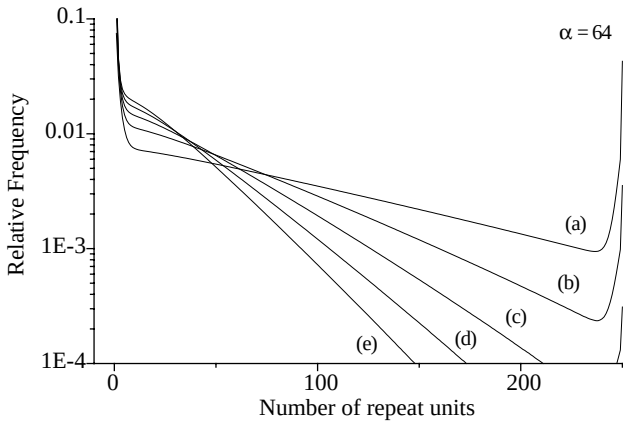

Fig. 6. Frequency distributions for $\alpha=64$, UID with $\chi_0=250$. (a) $\tau=0.008$, (b) $\tau=0.016$, (c) $\tau=0.025$, (d) $\tau=0.033$, (e) $\tau=0.044$.

Here species are lost only from the ends of molecules. Note that this is fundamentally different from the conventional ECS model, considered in an earlier paper [9], where the rate at which monomers are lost is independent of the molecule size and just depends on the number of molecules in the population.

It can be shown from the exact solution, or by direct solution of the population balance equations, that for a UID, the frequency distribution for pure ECS follows essentially a binomial distribution,

$$\frac{N_i(\tau)}{N(0)}=\begin{cases}(n-1)(1-\mathrm{e}^{-\tau})+(1-\mathrm{e}^{-\tau})^{n-1}, & i=1\\ {}^{n-1}C_{i-1}(1-\mathrm{e}^{-\tau})^{n-i}\mathrm{e}^{-(i-1)\tau}, & 2\leq i<n\\ \mathrm{e}^{-(n-1)\tau}, & i=n\end{cases} \tag{19}$$

where ${}^{(n-1)}C_{i-1}$ is the binomial coefficient. Now when n is large, the term $(1-\mathrm{e}^{-\tau})^{n-1}$ may be neglected in the expression for N_1, except when $\tau\to\infty$. Comparison with Eq. (7) then shows that for large n, $N_1(\tau)/N(0)\approx N(\tau)/N(0)-1$, and so it follows that the number of monomers will be much greater than the frequency of any other molecule in the distribution for $0<\tau<\infty$. Hence, for large n, if volatilisation occurs such that monomers are removed instantaneously, then the remaining mass will be given to a good approximation by

$$\frac{\mu_1^{(m_v)}}{\mu_1}\approx 1-\frac{N_1(\tau)}{\mu_1}\approx \mathrm{e}^{-\tau} \tag{20}$$

and will be independent of the particular choice of m_v. Furthermore, given the observations made above, we should also expect the remaining mass to be approximately independent of the initial distribution provided that the initial average degree of polymerisation is large. Note that this is in direct contrast to the conventional view of ECS covered in an earlier paper [9], where the degradation rates do not depend on the number of bonds in the molecule (and hence the size of the molecule), and the expected variation of remaining mass with τ does depend on the initial degree of polymerisation and is given by $\mu_1^{(m_v)}/\mu_1\approx 1-\tau/\chi_0$.

Fig. 7 shows the effect of α on the remaining mass as a function of time, taking $m_v=10$. This shows that for fixed k, the model predicts that the effect of increasing RS is to increase the

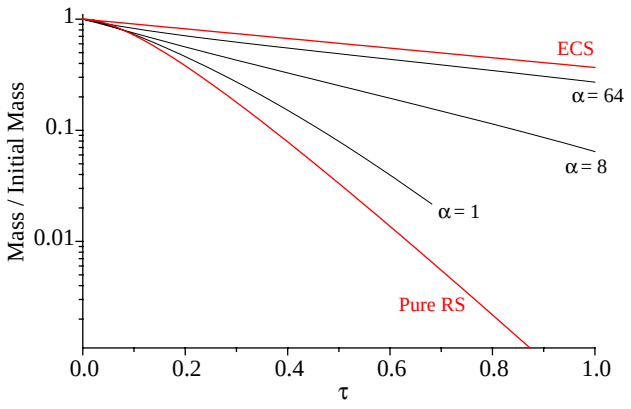

Fig. 7. Effect of exponent on mass loss ($\lambda = 10$).

rate at which volatile products are produced compared with ECS.

3.3. Break-at-a-point

The effect of a bond breaking at a particular location within a molecule may also be investigated within this framework. This would correspond in practice to a molecule with a weak point located at a consistent point along its length. Let $0 < \theta \leq 0.5$ represent the fractional position along the length of a molecule at which scission is to occur. Now, for a j-mer, this implies that the bond b closest to $\theta(j-1)$ will break. Let x be a real number and let int(x) denote the integer part of x (so that int(e) = 2, int(π) = 3, etc.). Then let $\varepsilon = \theta(j-1) - \text{int}(\theta(j-1))$ and define b as

$$b = \begin{cases} 1 & \text{if } \theta(j-1) < 1 \\ \text{int}(\theta(j-1)) & \text{if } \varepsilon < 0.5 \\ 1 + \text{int}(\theta(j-1)) & \text{if } \varepsilon \geq 0.5 \end{cases} \quad (21)$$

Accordingly we define

$$w_i^{(j)} = \begin{cases} 0 & \text{if } i \neq b \\ 1 & \text{if } i = b \text{ and } b = j-b \\ 0.5 & \text{if } i = b \text{ or } i = j-b \text{ and } b \neq j-b \end{cases} \quad (22)$$

The graph in Fig. 8 shows the computed relative frequency

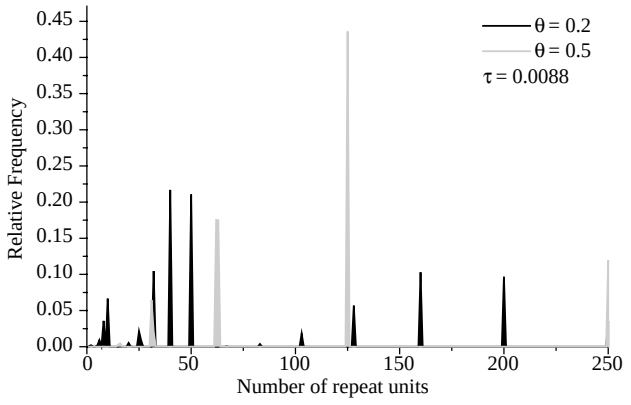

Fig. 8. Relative frequency plots at $\tau = 0.0088$ for $\theta = 0.2, 0.5$.

distributions for a UID ($\chi_0 = 250$) at a fixed value of τ for $\theta = 0.2$ and 0.5. Note that the frequency shows abrupt peaks at appropriate fractions of the initial degree of polymerisation (corresponding to $\theta^j\chi_0$ and $(1-\theta)^j\chi_0$ for integer values of j).

The graph in Fig. 9 shows the effect of θ on the remaining mass (with $m_v = 10$) as well as the relative frequencies at $\tau = 0.1, 0.2, 0.3, 0.4$ for the $\theta = 0.5$ case.

4. Application to the thermal degradation of PMMA

Consider an experiment involving a polymer degrading by pure ECS and let (t_{exp}, T_{exp}, M_{exp}) represent the observed time, temperature and ratio of mass/initial mass, respectively. Eq. (20) above suggests that τ may be calculated from the experimental data by defining $\tau = -1\text{n}\, M_{exp}$ and then k may be found from $k(T_{exp}) = -\text{d}(\ln M_{exp})/\text{d}t_{exp}$.

TG experiments in nitrogen on PMMA samples of two different initial molecular weights were carried out. The polymer samples were obtained from Polymer Laboratories (UK) inc. with molecular weights 10,260 and 49,600 g mol^{-1}, respectively (part nos. 2022-9001, 2023-3001, batch nos. 20229-10, 20233-11). In both cases the PMMA molecules were terminated by diphenyl hexyl units. The heating curves for the experiments are shown in Fig. 10 (the lighter molecular weight sample was subjected to the grey heating curve and the heavier sample was subjected to the black curve). The experimental data were used to construct k as indicated above, and the results are shown in the Arrhenius plot of Fig. 11. This plot indicates that to a leading order, k does not depend strongly on the initial molecular weight of the samples. A least squares fit to this data gave the parameter values $J = 14.15$, $T_A = 12{,}668$ K. Note that there is some evidence in the lower molecular weight data of two mass loss processes occurring—an observation already well known from previous experimental studies [19,20].

The graph in Fig. 12 compares model predictions for the remaining mass (using the Arrhenius parameters found above) with TG data for the two different experiments. The symbols correspond to the TG data and the curves to the predicted mass fractions.

Previous isothermal studies with PMMA [16–18] have shown that there is a dependence of the observed degradation rate k_{obs} on initial molecular weight which the pure ECS model does not predict, nor is it clear from Fig. 11 that this is the case. Therefore, a third experiment was carried out using PMMA with initial molecular weight 518,900 g mol^{-1} (part number 2023-9001, batch number 20239-7, supplied by Polymer Laboratories, also terminated by diphenyl hexyl units). The heating curve was the same as for the 49,600 g mol^{-1} sample.

The results, shown in Fig. 13, indicate that k_{obs} does indeed depend on initial molecular weight for the higher MW sample. Also from this figure, the solution of $14.14 - 12{,}668/T = 23.85 - 19{,}318/T$ shows that when $T < 686$ K, k_{obs} increases with $1/\chi_0$ and when $T > 686$ K, k_{obs} decreases with $1/\chi_0$. This observation agrees well with the data of Barlow et al. [16], where they found a transition from k_{obs} increasing with $1/\chi_0$ to k_{obs} decreasing with $1/\chi_0$ at some temperature between 673 and

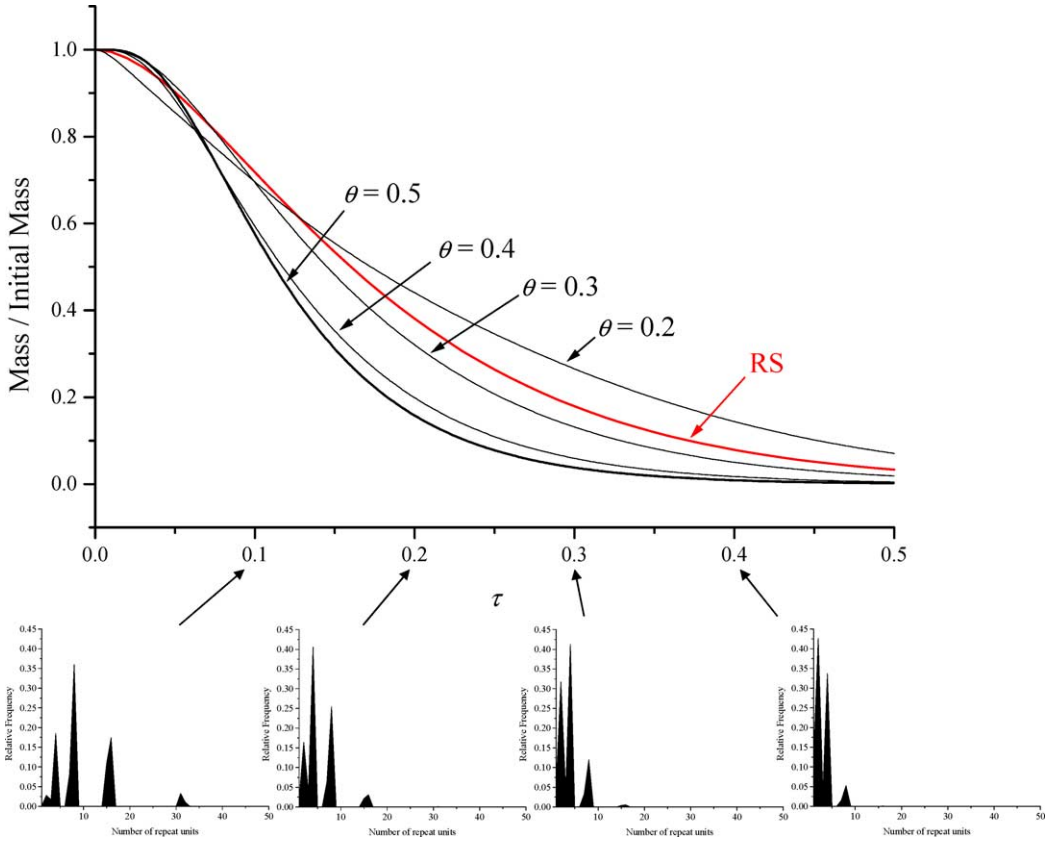

Fig. 9. Effect of breakage point on remaining mass ($m_v = 10$) with frequency plots for $\theta = 0.5$.

705 K (however, it should be noted that Holland and Hay [15] noted a similar transition at a temperature between 643 and 673 K).

The discrepancy between the observed dependence of k_{obs} on $1/\chi_0$ with the predictions of the pure ECS model may be due to a lack of detail included in the pure ECS model. For example, the model makes no distinction between a radical fragment and a molecule and so no termination processes are explicitly modelled. However, it has also been suggested, based on isothermal studies [15–18], that RS plays an increasingly important role in the thermal degradation of PMMA, depending on the temperature, and that this in turn affects the nature of the dependence of degradation rate on initial molecular weight. In order to investigate this situation, we now construct an approximation for k_{obs} for the end-bond weighted case (17) above, which represents a degradation process involving a simultaneous mixture of RS and ECS. Consider the behaviour of the general bond-weighted solution for small τ (the initial slope of the mass loss curve may be used to estimate k_{obs}). When τ is small, Eq. (3) above for a UID gives

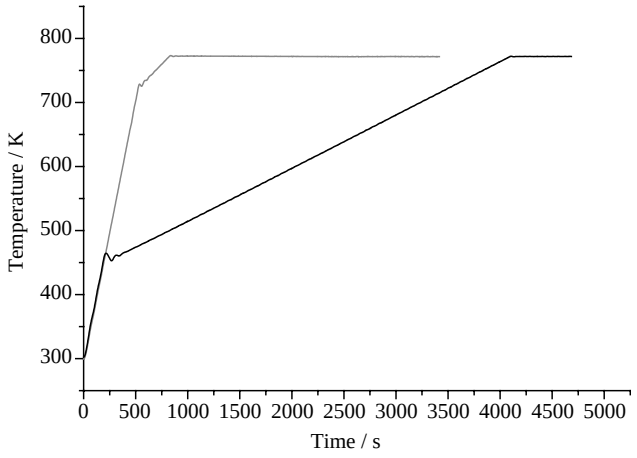

Fig. 10. Temperature–time curves used in TG experiments.

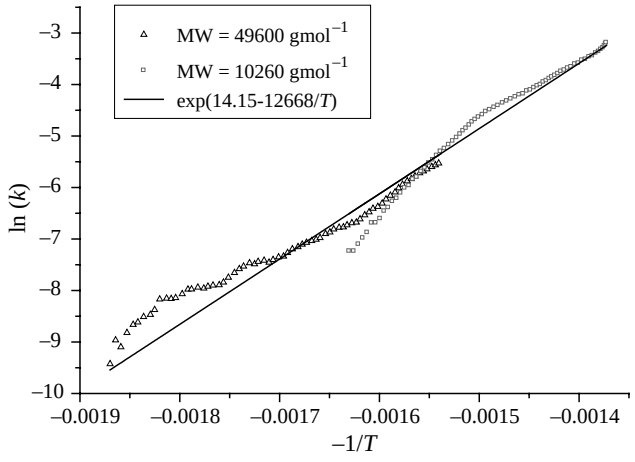

Fig. 11. Arrhenius plot of PMMA TG data.

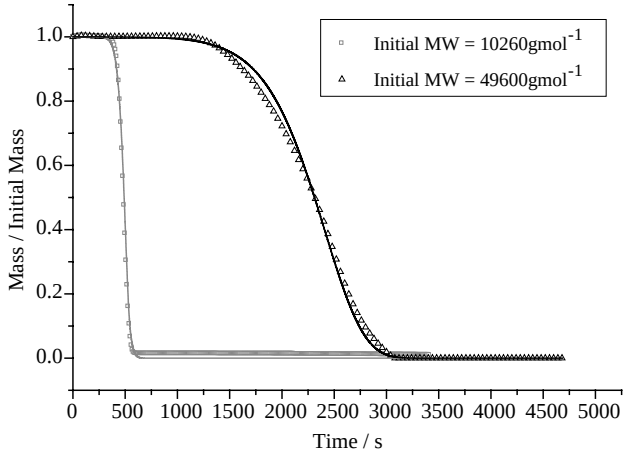

Fig. 12. Comparison of model predictions (curves) with experimental TG results (symbols) for PMMA.

$$\frac{N_i}{N(0)} = \begin{cases} (n-1)(w_{n-i}^{(n)} + w_i^{(n)})\tau + O(\tau^2), & i = 1,2,\ldots,n-1 \\ 1-(n-1)\tau + O(\tau^2), & i = n \end{cases} \tag{23}$$

Using these expressions, it follows that

$$\frac{\mu_1^{(m_v)}}{\mu_1} = 1 - \left(\frac{n-1}{n}\right)\left\{n - \sum_{i=m_v}^{n-1} i\left(w_{n-i}^{(n)} + w_i^{(n)}\right)\right\}\tau + O(\tau^2) \tag{24}$$

Thus, if k_{ECS} is the degradation rate for pure end-chain scission, for isothermal conditions it follows that

$$\frac{k_{obs}}{k_{ECS}} \approx n - 1 - \left(\frac{n-1}{n}\right)\sum_{i=m_v}^{n-1} i\left(w_{n-i}^{(n)} + w_i^{(n)}\right) \tag{25}$$

Now, taking the weights given in Eq. (17) for end-bond weighted scission, it may be shown from the expression above that for large n,

$$\frac{k_{obs}}{k_{ECS}} \approx 1 + \frac{m_v(m_v-1) - \chi_0}{\chi_0 + 2(\lambda - 1)} \tag{26}$$

Recall that when $\lambda = 1$, the case of pure RS is recovered and as

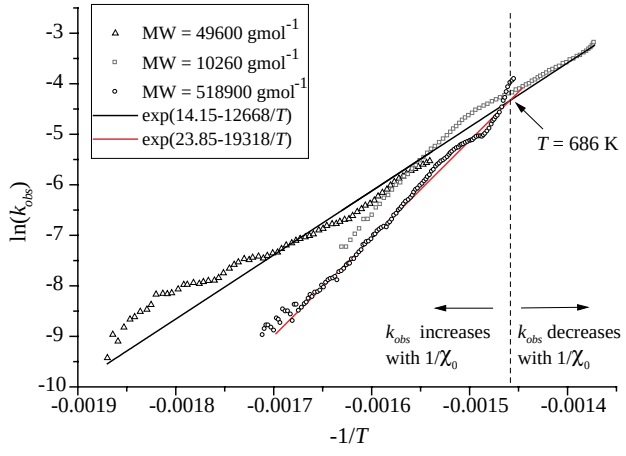

Fig. 13. Initial molecular weight dependence of degradation rate.

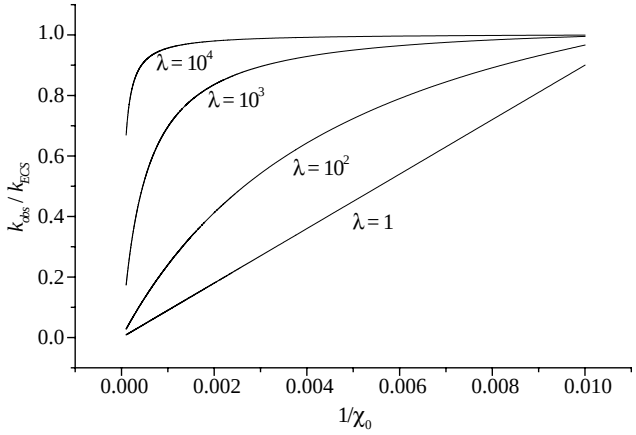

Fig. 14. Predicted variation of k_{obs}/k_{ECS} from end-bond weighted scission.

$\lambda \to \infty$ the case of pure ECS is recovered. Therefore, when there is simultaneous RS and ECS, the end-bond weighted model predicts that k_{obs} will increase with $1/\chi_0$. The graph in Fig. 14 shows the variation of k_{obs}/k_{ECS} with $1/\chi_0$ for $m_v = 10$. Note that these results suggest that the relationship between k_{obs} and is linear only for the case of pure random scission and also that increased ECS (increasing λ) has the effect of reducing the slope of the curve for moderate values of $1/\chi_0$.

Note also that an alternative method of incorporating RS into the overall degradation mechanism would be to view pure ECS and RS as separate parallel reactions, each with its own distinct rate constant. If one does this, then it may be shown that the effect on k_{obs} is to replace Eq. (26) by the expression

$$\frac{k_{obs}}{k_{ECS}} = 1 + \frac{m_v(m_v-1)}{\chi_0}\frac{k_{RS}}{k_{ECS}} \tag{27}$$

Clearly this is always a linear function of $1/\chi_0$ unless k_{RS} is zero. In order to reproduce the observed experimental behaviour up to the transition where k_{obs} reduces with $1/\chi_0$, the ratio k_{RS}/k_{ECS} would have to be a decreasing function of temperature, again implying that ECS plays an increasingly dominant role as temperature increases.

Returning to Fig. 13, it is apparent that the variation of k_{obs} with $1/\chi_0$ reduces as temperature increases up to 686 K. The result above then suggests that this behaviour is consistent with a simultaneous combination of RS and ECS at low temperature, with ECS playing an increasingly dominant role as temperature increases up to 686 K. The results of Barlow et al. [16] also show this behaviour, although they reach a different conclusion as to the relative importance of the scission mechanisms. Holland and Hay [15] also reached this conclusion, but by a fundamentally different route based on the kinetic model of Lehrle et al. [21].

As temperature increases still further, Fig. 13, Holland and Hay's results [15] and those of Barlow et al. [16] show that k_{obs} reduces with $1/\chi_0$, which is not predicted by the end-bond weighted model and so this behaviour is consistent with the view that a separate scission process must be occurring. Consideration of the experimental evidence suggests that at higher temperatures, thermal degradation rates for all i-mers are not the same and so the simplification made initially, that

$k_i = k$ for all i, becomes invalid. In fact, it would appear that at higher temperatures k_i becomes an increasing function of i. Hence a first-order correction to account for this process might take the form

$$k_i = k + \left(\frac{i-1}{\chi^*}\right)^{\beta} k^* \tag{28}$$

where k^*/k is small for temperatures below the transition, χ^* is a critical degree of polymerisation and β is a characteristic exponent. It may be shown that application of this correction to the end-bond weighted model for a UID results in the following approximate expression for k_{obs}/k_{ECS}:

$$\frac{k_{obs}}{k_{ECS}} \approx \left\{1 + \frac{k^*}{k_{ECS}}\left(\frac{\chi_0}{\chi^*}\right)^{\beta}\right\}\left\{1 + \frac{m_v(m_v-1)-\chi_0}{\chi_0 + 2(\lambda-1)}\right\} \tag{29}$$

Note that in order for k_{obs} to be a decreasing function of $1/\chi_0$ for some value of k^*/k_{ECS}, it is necessary to take $\beta \geq 1$. For the sake of illustration, if we set $\lambda = 50$, $m_v = 10$, $\chi^* = 100$, $\beta = 1$, then the behaviour in Fig. 15 results, which qualitatively agrees with the observed behaviour.

The kinetic approach of Lehrle et al. [21], where explicit termination reactions are included leads to an expression of the form

$$\frac{k_{obs}}{k_{ECS}} = \left(\frac{2k_{RS}}{k_{ECS}} + \frac{1}{\chi_0}\right)Z$$

for first-order termination, where Z is the ratio of the rate constants for beta-scission and termination. This expression arises through the assumption that there is only one reactive site per molecule chain leading to the formation of monomers and that random scission of a chain creates two chain fragments. Note that this expression predicts that in the absence of any RS events, k_{obs} will be directly proportional to $1/\chi_0$.

It is important to understand that this approach views the scission events in an entirely different manner to the present approach. Here, the number of scission events depends on the number of bonds in the molecule, implying that the rate of monomer formation will also depend not just on the number, but also on the size of the molecules present in the population.

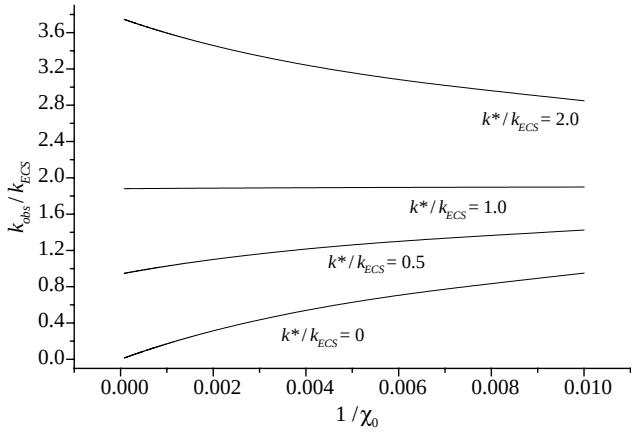

Fig. 15. Variation of k_{obs}/k_{ECS} for modified end-bond weighted scission.

It is this property of the bond-weighted approach that leads to the observation made in Section 3.2 that when the probability of an end bond breaking is much greater than the probability of any other bond in the molecule breaking (pure ECS) then k_{obs} will not depend on χ_0. In fact, if the traditional view of ECS is adopted, where there is only one reactive site per molecule, then application of population balance theory leads to a case that has already been covered by the author in an earlier paper [9]. In this case it transpires that k_{obs} is directly proportional to $1/\chi_0$, in accord with the model of Lehrle et al.

5. Conclusion

The discrete bond-weighted population balance model offers an extension over existing discrete population balance models and provides a framework in which a number of scission processes may be studied, including pure random scission, end-chain scission, simultaneous combination of end-chain and random scission, as well as more unusual mechanisms such as break-at-a-point scission.

Adopting a simple view of volatilisation, where molecules with fewer than m_v repeat units volatilise as soon as they are formed, it is possible to derive exact solutions for the remaining mass for end-chain scission and pure random scission. It was found that the volatilisation rate does not depend on the initial distribution of molecules or m_v for end-chain scission, and depends only on m_v and the number average degree of polymerisation of the initial distribution for pure random scission. Comparison of the pure random scission model with experimental thermogravimetric data (both isothermal and constant heating rate) gave reasonable agreement for polyethylene of relatively low initial molecular weight.

Comparison of the end-chain scission model with thermogravimetric data for PMMA of relatively low initial molecular weight showed good agreement. However, for higher molecular weights, it was found that simple pure end-chain scission was insufficient to explain the results. This discrepancy may be due to the fact that the scission model considered here is insufficiently detailed, however, previous experimental studies have suggested that random scission plays an important role in the thermal degradation of PMMA and with this in mind, a form of the bond-weighted model incorporating simultaneous end-chain and random scission was investigated. It was found that simultaneous random scission and end-chain scission is sufficient to explain the observed degradation rates at lower temperatures provided that end-chain scission becomes increasingly dominant as temperature increases. This observation is in agreement with conclusions reached by previous workers [15] where a traditional kinetic model is used to interpret the experimental data. However, at higher temperatures experimental studies show that observed degradation rates increase with initial degree of polymerisation—a feature not predicted by the end-bond weighted model. Further consideration suggested that the discrepancy might arise from an initial simplification, where the degradation rates were assumed to be independent of the size of the molecule. It was

found that a correction to the degradation rate which involved adding a temperature-dependent term, which is an increasing function of molecule size could qualitatively reproduce the observed dependence of degradation rate with initial degree of polymerisation at higher temperatures.

References

[1] McCoy BJ, Madras G. Evolution to similarity solutions for fragmentation and aggregation. J Colloid Interface Sci 1998;201:200.

[2] McCoy B. Distribution kinetics for temperature-programmed pyrolysis. Ind Eng Chem Res 1999;38:4531.

[3] McCoy B. Polymer thermogravimetric analysis: effects of chain-end and reversible random scission. Chem Eng Sci 2001;56:1525.

[4] Madras G, McCoy B. Numerical and similarity solutions for reversible population balance equations with size-dependent rates. J Colloid Interface Sci 2002;246:356.

[5] McCoy BJ, Madras G. Discrete and continuous models for polymerization and depolymerization. Chem Eng Sci 2001;56:2831.

[6] Staggs JEJ. A continuous model for vaporisation of linear polymers by random scission and recombination. Fire Saf J 2005;40:610.

[7] Kostoglou M. Mathematical analysis of polymer degradation with end-chain scission. Chem Eng Sci 2000;55:2507.

[8] Staggs JEJ. Modelling random scission of linear polymers. Polym Degrad Stab 2002;76:37.

[9] Staggs JEJ. Modelling end-chain scission and recombination of linear polymers. Polym Degrad Stab 2004;85:759.

[10] Yoon JS, Jin HJ, Chin IJ, Kim C, Kim MN. Theoretical prediction of weight loss and molecular weight during random chain scission degradation of polymers. Polymer 1997;38:3573.

[11] Inaba A, Kashiwagi T. A calculation of thermal degradation initiated by random scission, unsteady radical concentration. Eur Polym J 1987; 23:871.

[12] Emsley AM, Heywood RJ. Computer modelling of the degradation of linear polymers. Polym Degrad Stab 1995;49:145.

[13] Platkowski K, Reichart K-H. Application of Monte Carlo methods for modelling of polymerization reactions. Polymer 1999;40:1057.

[14] Bose SM, Git Y. Mathematical modelling and computer simulation of linear polymer degradation: simple scissions. Macromol Theory Simul 2004;13:453.

[15] Holland BJ, Hay JN. The kinetics and mechanisms of the thermal degradation of poly(methyl methacrylate) studied by thermal analysis-Fourier transform infrared spectroscopy. Polymer 2001; 42:4825.

[16] Barlow A, Lehrle RS, Robb JC, Sunderland D. Polymethylmethacrylate degradation—kinetics and mechanisms in the temperature range 340° to 460 °C. Polymer 1967;2:527.

[17] Bagby G, Lehrle RS, Robb JC. Kinetic measurements by micropyrolysis-GLC: thermal degradation of polymethylmethacrylate possessing laurylmercaptyl end groups. Polymer 1969;10:683.

[18] Lehrle RS, Atkinson D, Cook S, Gardner P, Groves S, Hancox R, et al. Polymer degradation mechanisms: new approaches. Polym Degrad Stab 1993;42:281.

[19] Kashiwagi T, Inaba A, Brown JE, Hatada K. Effects of weak linkages on the thermal and oxidative degradation of poly(methyl methacrylates). Macromolecules 1986;19:2160.

[20] Peterson J, Vyazovkin S, Wight C. Kinetic study of stabilizing effect of oxygen on thermal degradation of poly(methyl methacrylate). J Phys Chem B 1999;103:8087.

[21] Lehrle RS, Peakman RE, Robb JC. Pyrolysis-gas-liquid-chromatography utilised for a kinetic study of the mechanisms of initiation and termination in the thermal degradation of polystyrene. Eur Polym J 1982;18:529.